Increase of Autonomic Nerve Factors in Epicardial Ganglionated Plexi During Rapid Atrial Pacing Induced Acute Atrial Fibrillation

Authors' Contribution:
Study Design A
Data Collection B
Statistical Analysis C
Data Interpretation D
Manuscript Preparation E
Literature Search F
Funds Collection G

BCDEFG Yang Li*
BCDEFG Yan-Mei Lu*
G Xian-Hui Zhou
G Ling Zhang
G Yao-Dong Li
G Jiang-Hua Zhang
G Qiang Xing
A Bao-Peng Tang

Department of Cardiology, First Affiliated Hospital, Xinjiang Medical University, Urumqi, Xinjiang, P.R. China

* These authors contributed equally to this work and should be considered co-first authors
Corresponding Author: Bao-Peng Tang, e-mail: tangbaopeng1111@163.com
Source of support: This work was supported by the National Natural Science Foundation of China (NSFC81260037, NSFC81660071)

Background: The cardiac autonomic nervous system plays an essential role in epicardial ganglionated plexi (GP) regulation of atrial fibrillation onset and progression. To date, the activity of GP and the function of the cardiac autonomic nervous system are not well understood. The aim of this study was to determine alterations in epicardial GP cholinergic nerve, adrenergic nerve, and nerve growth factor expression using rapid atrial pacing to induce atrial fibrillation in canines.

Material/Methods: Nine healthy adult beagles were divided into two groups: the pacing experimental group (n=6) and the sham-operation control group (n=3). For the pacing group, high frequency pacing of the left atrial appendage was performed for eight hours. In the control group, electrodes were implanted without rapid atrial pacing. Immunocytochemistry was used to identify neurons positively expressing tyrosine hydroxylase, choline acetyl transferase, nerve growth factor and neurturin.

Results: After successfully establishing a rapid atrial pacing of the left atrial appendage induced atrial fibrillation model, we found that expression of choline acetyl transferase, tyrosine hydroxylase, nerve growth factor, and neurturin was significantly higher in the rapid atrial pacing group than the control group ($p<0.05$).

Conclusions: In our model, incremental excitability of both the adrenergic and cholinergic nerves led to frequent incidents of atrial fibrillation, which were possibly due to an imbalance of autonomic nerve factors in the epicardial GP during acute atrial fibrillation.

MeSH Keywords: Atrial Fibrillation • Autonomic Nervous System • Ganglia, Autonomic

Full-text PDF: http://www.medscimonit.com/abstract/index/idArt/902621

📄 2691   ▦ —   📊 7   📑 31

Background

Atrial fibrillation is a common clinical arrhythmia that may cause fatal complications such as cerebral apoplexy and heart failure. Patients with atrial fibrillation are at increased risk for the development of cardiovascular disease, thereby severely undermining health and overall well-being [1–3]. Because of the complexity of the pathogenesis underlying atrial fibrillation, there are few effective therapies available. Recent studies have found that the cardiac autonomic nervous system, which participates in the formation and transmission of cardiac impulses, plays an important role in the occurrence and development of atrial fibrillation [4,5].

The cardiac autonomic nervous system is composed of the extrinsic cardiac autonomic nervous system and the intrinsic cardiac autonomic nervous system. The intrinsic cardiac autonomic nervous system is a neural network that consists of epicardial ganglionated plexi (GP) and the ligaments of Marshall [6–8]. Rather than functioning merely as a transition station for neural signals, GP can independently intervene in cardiac physiological functions as a signal integration and regulation system. Therefore, GP are known as the "integration centers" of neural networks [9,10]. Additionally, in animal experiments, it has been shown that stimulating and blocking GP can induce and eliminate focal impulses, respectively, that originate from the pulmonary vein area [11–13]. Ablating primary GP has been shown clinically to improve the success rates of atrial fibrillation treatment with pulmonary vein sequestration [14,15]. Although these studies suggested that focal impulses in the cardiac autonomic nervous system originated from both pulmonary vein and non-pulmonary vein areas, activity of GP during the occurrence and development of atrial fibrillation remains unclear. Here, we studied changes in the level of autonomic nerve factors of GP in atrial fibrillation in an eight hour rapid atrial pacing induced canine model of atrial fibrillation.

Material and Methods

Animal preparation

This study was carried out in strict accordance with the recommendations established in the Guide for the Care and Use of Laboratory Animals of the National Institutes of Health. The animal use protocol was reviewed and approved by the Institutional Animal Care and Use Committee of Xinjiang Medical University, China. In total, nine healthy adult beagles, both male and female, one to two years old, weighing 12.0±1.5 kg, were obtained from the First Affiliated Hospital of Xinjiang Medical University Animal Center. Sodium pentobarbital was administered intravenously for anesthesia (initial bolus

30 mg/kg, 50–100 mg as necessary for maintenance). All dogs were given a ventilator in a room with air circulation and positive pressure, and an insulation blanket was used to maintain the body temperature at 36.5±1.5°C. The chest was entered via left thoracotomy at the fourth intercostal space. For pacing, several 10-bipolar electrodes were sutured using a non-injurious method at the left atrial appendage. Electrocardiogram and basic vital signs, such as oxygen saturation and arterial blood pressure, were monitored throughout the duration of the experiment.

Canine acute atrial fibrillation model

Canine acute atrial fibrillation model was generated as described previously by Lu et al. [16]. The left atrial appendage was sutured with electrodes with a pacing frequency of 1,200 times/minute and pacing voltage set at two times that of the pacing threshold. For the rapid atrial pacing group, high frequency pacing of the left atrial appendage was performed for eight hours. In the sham-operation control group, surgery was performed as described except for administration of rapid atrial pacing. All program aspects were measured using electrodes connected to the heart from a multiconductive polygraph (Lead-7000 EP Control, Sichuan Jinjiang, China).

Epicardial GP

Localization of GP was conducted according to protocols previously described [17] (Figure 1). Distribution of primary GP was as follows: anterior right ganglionated plexus (ARGP) was located between the anterior right pulmonary vein and the inferior right pulmonary vein, near the pulmonary vein ostium; inferior right ganglionated plexus (IRGP) was located at the juncture of the inferior vena cava and the atrium; superior left ganglionated plexus (SLGP) was located between the inferior left pulmonary vein and the left pulmonary artery; inferior left ganglionated plexi (ILGP) was located at the junction of the inferior left pulmonary vein and the inferior posterior wall of the left atrium; and other GP were located within the ligaments of Marshall.

Histology

After completion of the experiment, canine myocardial tissue from each group was dissected and fixed in 4% paraformaldehyde for at least 24 hours and stored in 70% ethanol. The samples were desiccated and embedded in paraffin prior to being cut into 5 µm sections. Sections were then processed for hematoxylin and eosin (H&E) staining and Masson's trichrome staining.

Masson's trichrome staining

The sections were dewaxed and stained in Masson's compound staining solution for five minutes. Then, they were washed with
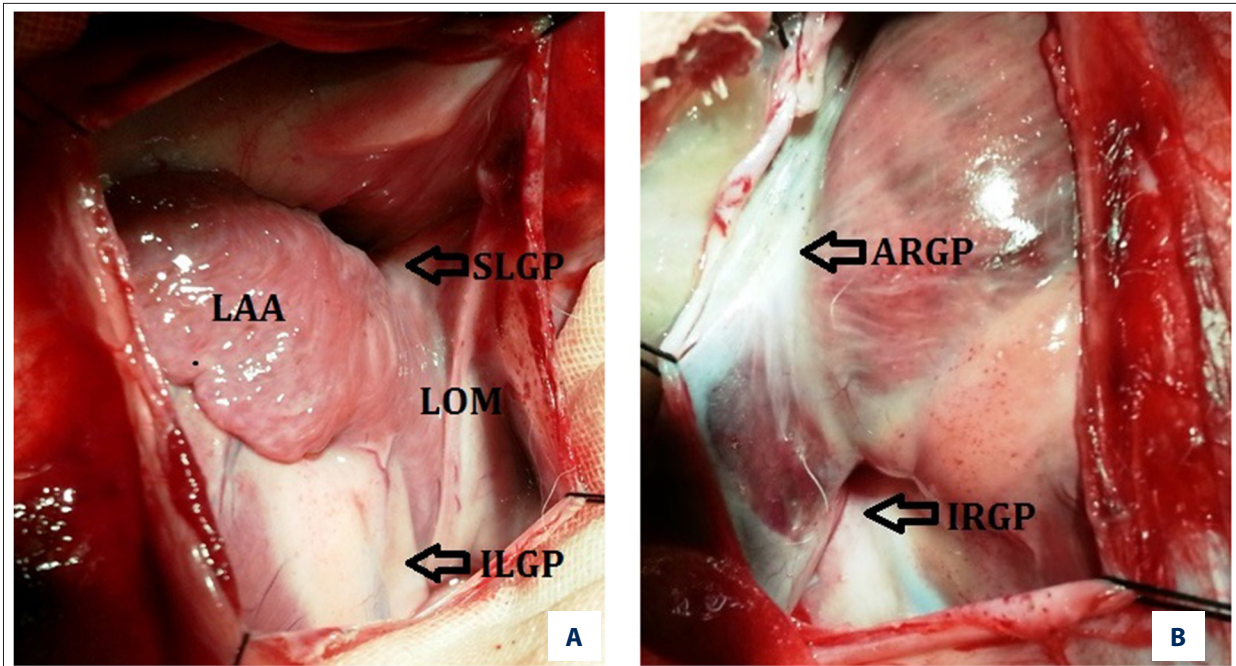
Figure 1. Left and right GP. (**A**) Left GP, SLGP+LOM+ILGP; (**B**) Right GP, ARGP+IRGP. Each GP shows a faint yellow adipose tissue covering on the myocardial tissues. ARGP – anterior right ganglionated plexi; IRGP – inferior right ganglionated plexi; SLGP – superior left ganglionated plexi; ILGP – inferior left ganglionated plexi; LOM – ligament of Marshall.

0.2% acetic acid solution, processed with 5% phosphomolybdic solution for five to ten minutes, treated twice with 0.2% acetic acid solution, stained with aniline blue for five minutes, treated twice with 0.2% acetic acid solution, desiccated with absolute ethyl alcohol, vitrified by dimethylbenzene, and sealed and deposited in neutral balsam. After staining, the sections were visualized using a DM3000 Leica microscope (Wetzlar, Germany) and imaged.

Immunohistochemistry of nerve fibers and quantitative analysis of fiber density

Sections were dewaxed, and antigens were repaired at the defrosting degree of sodium citrate, cooled, and then reacted with 3% H_2O_2 for 10 minutes to block endogenous peroxidases. Sections were incubated with the following primary antibodies (1: 100, Rabbit Anti-, Bioss, Woburn, MA, USA) overnight: tyrosine hydroxylase, choline acetyl transferase, nerve growth factor, and neurturin. Sections were then incubated with horseradish peroxidase conjugated secondary antibody. The sections were rinsed with phosphate buffered saline between each step. Finally, fluorescence was developed using a diaminobenzidine kit. Image-Pro Plus 6.0 (Media Cybernetics, Rockville, MD, USA) was used to determine the nerve density. The computer automatically detected developed autonomic nerves and calculated the pixel area of the developed nerves. The nerve density was defined as the entire detection area divided by the nervous area ($\mu m^2/mm^2$). Each section was observed 40 times per eyepiece, and the three densest visual fields were selected. Average density was used to denote nerve density of a given section.

Statistical analysis

All data are presented as the mean ± deviation, and data analyses were performed with SPSS 13.0 (Chicago, IL, USA). Intra-group comparisons were performed using an independent samples t-test. A value of $p<0.05$ was considered statistically significant.

Results

Establishment of canine atrial fibrillation model

As the pacing time was prolonged, so was the number of spontaneous atrial fibrillation incidents. Surface electrocardiogram measurements demonstrated unordered electrical activity. Rather than P waves, f waves with varying amplitudes, intervals, and patterns were solely observed for over 10 second periods. The frequency was 450–600 times/minute and the R-R interval varied. As seen in Figure 2, the canine atrial fibrillation model was successfully established.
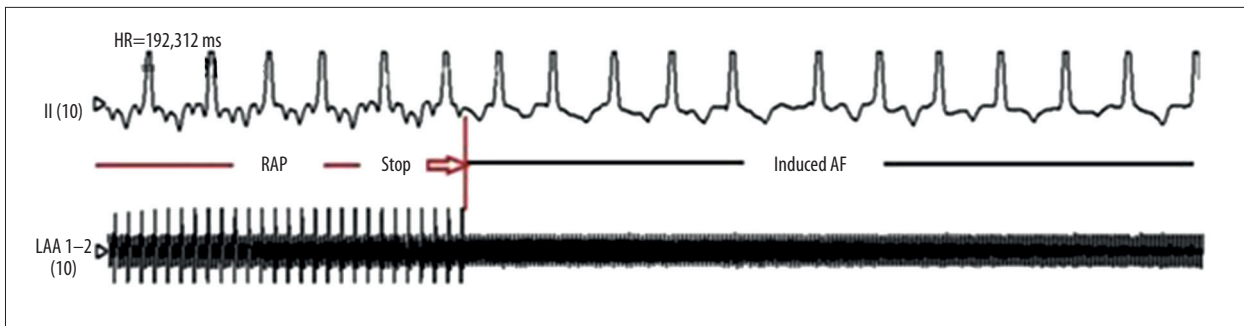
Figure 2. Rapid atrial pacing induced atrial fibrillation. Red arrow denotes the termination of rapid atrial pacing; subsequently, spontaneous atrial fibrillation was observed. P waves disappeared, and f waves were observed with varying amplitudes, intervals, and patterns. The frequency was 450–600 times/minute and R-R interval varied.
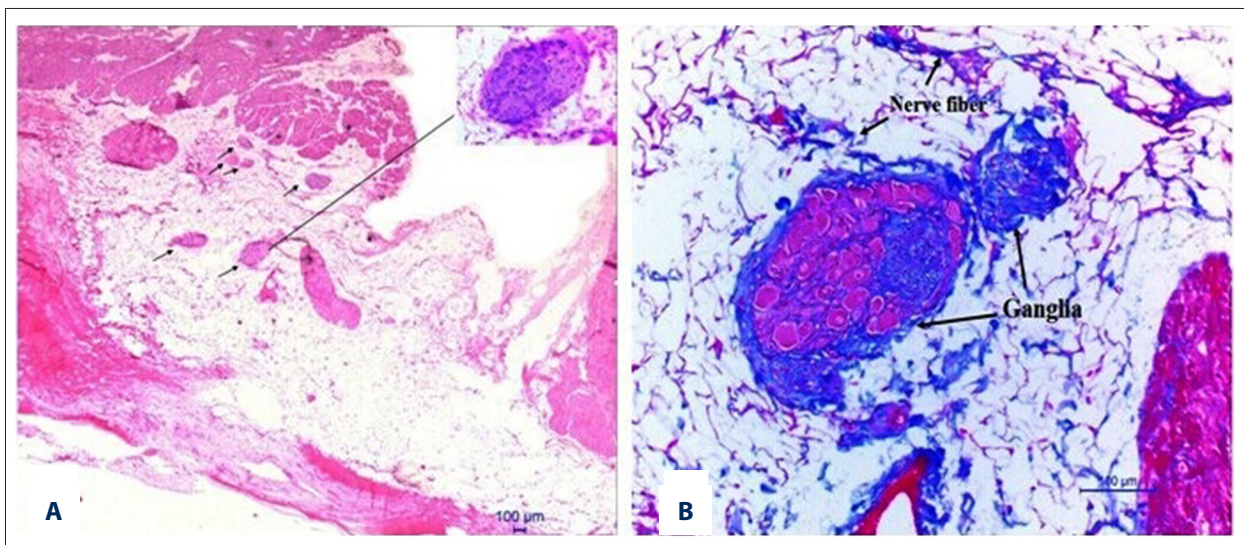
Figure 3. H&E and Masson's staining of ARGP. (**A**) H&E staining of ARGP ×10. Myocardial tissues and massive fat were observed. In adipose tissues, there were various ganglia, as indicated by the black arrows. The top right corner shows one amplified ganglion. (**B**) Masson's staining of ARGP ×20 ganglia. Black arrows indicate nerve fibers and ganglia.

## Morphology and distribution of epicardial GP

H&E staining revealed that the distribution of ganglia was localized to adipose tissues and myocardium and that ganglion cells were attracted to alkalinity. Ganglia had large diameters, were polygonal shaped and surrounded by satellite cells (Figure 3A). Masson's staining suggested that the ganglia consisted of various perikaryons and nerve fibers (Figure 3B).

Tyrosine hydroxylase and nerve growth factor immunoreactive neurons in GP

Immunohistochemistry was performed to identify tyrosine hydroxylase (a specific marker for adrenergic nerves) and nerve growth factor positive neurons in GP. In the sham operation control group, the density of tyrosine hydroxylase immunoreactive neurons in the ARGP, IRGP, SLGP, and ILGP were $(6.23\pm1.20)\times1,000$ $\mu m^2/mm^2$, $(7.56\pm1.28)\times1,000$ $\mu m^2/mm^2$, $(6.88\pm1.33)\times1,000$ $\mu m^2/mm^2$, and $(7.87\pm1.76)\times1,000$ $\mu m^2/mm^2$, respectively. In the rapid atrial pacing experimental group, the density of tyrosine hydroxylase immunoreactive neurons in the ARGP, IRGP, SLGP, and ILGP were $(18.98\pm4.36)\times1,000$ $\mu m^2/mm^2$, $(16.76\pm3.87)\times1,000$ $\mu m^2/mm^2$, $(17.43\pm3.76)\times1,000$ $\mu m^2/mm^2$, and $(16.85\pm4.33)\times1,000$ $\mu m^2/mm^2$, respectively. The difference in tyrosine hydroxylase positive neuron density between experimental group and control group was significantly different ($p<0.05$, see Figures 4 and 5).

The pacing group tyrosine hydroxylase ARGP/the sham-operation tyrosine hydroxylase ARGP=$(18.98\pm4.36)\times1,000$ $\mu m^2/mm^2/(6.23\pm1.20)\times1,000$ $\mu m^2/mm^2=3.04$. The pacing group tyrosine hydroxylase IRGP/the sham-operation tyrosine hydroxylase IRGP=$(16.76\pm3.87)\times1,000$ $\mu m^2/mm^2/(7.56\pm1.28)\times1,000$ $\mu m^2/mm^2=2.22$. The pacing group tyrosine hydroxylase SLGP/the sham-operation tyrosine hydroxylase SLGP=$(17.43\pm3.76)\times1,000$ $\mu m^2/mm^2/$
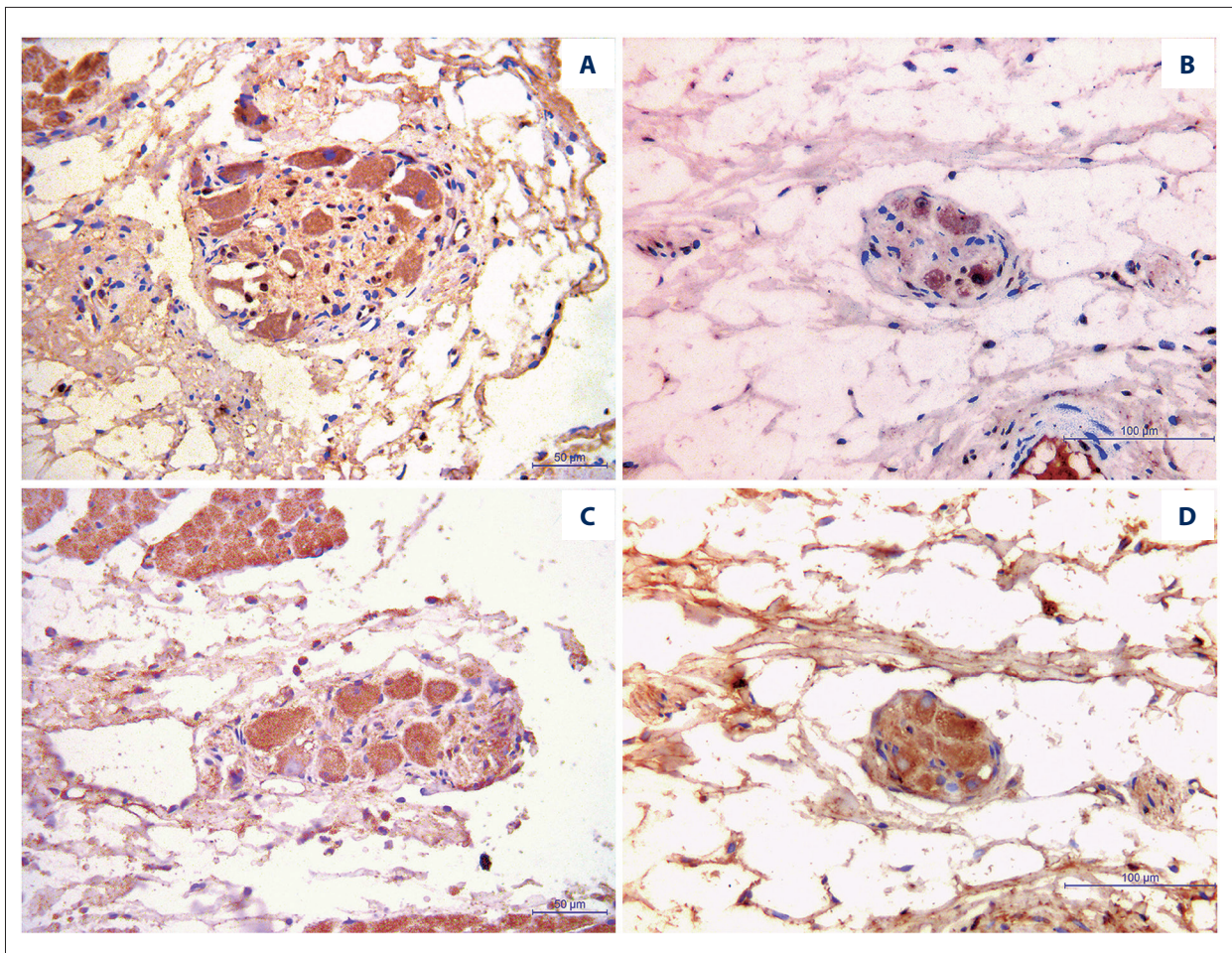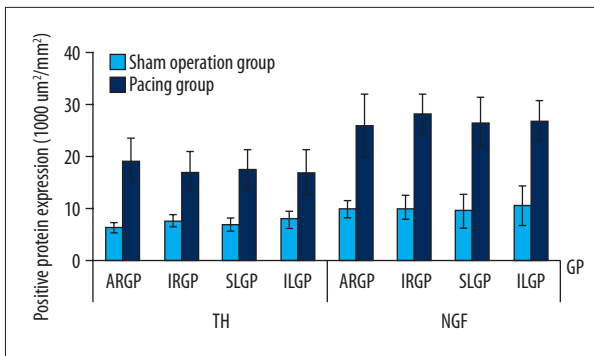
Figure 4. Comparison of tyrosine hydroxylase and nerve growth factor in ARGP between the control group and the rapid atrial pacing group. Blue is the nucleus, brown is positive staining. (**A**) Tyrosine hydroxylase staining of ARGP for the sham-operation control group. (**B**) Tyrosine hydroxylase staining of ARGP for the rapid atrial pacing group. (**C**) Nerve growth factor staining of ARGP for the sham-operation group. (**D**) Nerve growth factor staining of ARGP for the rapid atrial pacing group.

$(6.88\pm1.33)\times1,000$ μm²/mm²=2.53.The pacing group tyrosine hydroxylase ILGP/the sham-operation tyrosine hydroxylase ILGP=$(16.85\pm4.33)\times1,000$ μm²/mm²/$(7.87\pm1.76)\times1,000$ μm²/mm²=2.14.

In the sham operation group, the density of nerve growth factor (representative of the neurotrophic factor family) immunoreactive neurons in the ARGP, IRGP, SLGP, and ILGP were $(9.94\pm1.54)\times1,000$ μm²/mm², $(10.20\pm2.35)\times1,000$ μm²/mm², $(9.45\pm3.43)\times1,000$ μm²/mm², and $(10.56\pm3.70)\times1,000$ μm²/mm², respectively. In rapid atrial pacing group, the density of nerve growth factor immunoreactive neurons in the ARGP, IRGP, SLGP, and ILGP were $(25.76\pm6.24)\times1,000$ μm²/mm², $(28.09\pm3.89)\times1,000$ μm²/mm², $(26.45\pm4.88)\times1,000$ μm²/mm², and $(26.66\pm4.25)\times1,000$ μm²/mm², respectively The difference in the density of nerve growth factor neurons between experimental group and control group was significantly different ($p<0.05$, see Figures 4 and 5).

Choline acetyl transferase and neurturin expression in GP

Immunohistochemistry was used to identify choline acetyl transferase and neurturin positive neurons in GP. In the sham-operation control group, the density of choline acetyl transferase (a specific marker for cholinergic nerves) immunoreactive neurons in the ARGP, IRGP, SLGP, and ILGP were $(30.32\pm5.65)\times1,000$ μm²/mm², $(28.40\pm6.30)\times1,000$ μm²/mm², $(27.56\pm3.58)\times1,000$ μm²/mm², and $(31.87\pm4.13)\times1,000$ μm²/mm², respectively. In the rapid atrial pacing group, the density of choline acetyl transferase immunoreactive neurons in the ARGP, IRGP, SLGP, and ILGP were $(65.48\pm7.80)\times1,000$ μm²/mm², $(69.31\pm7.45)\times1,000$ μm²/mm², $(67.78\pm7.24)\times1,000$ μm²/mm², and $(65.30\pm6.83)\times1,000$ μm²/mm², respectively. There was a significant difference in choline acetyl transferase positive neuron density between experimental group and control group ($p<0.05$, see Figures 6 and 7).

Figure 5. For each GP, intra-group comparisons were statistically different ($p<0.05$).
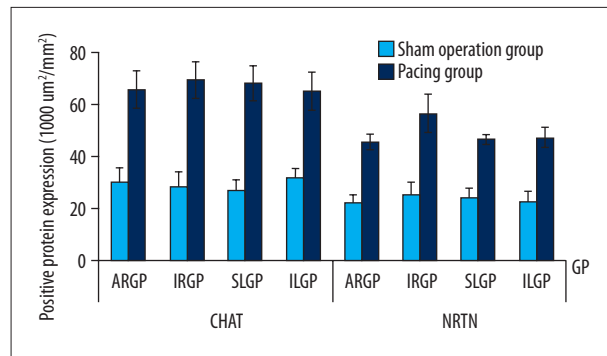
Figure 7. For each GP, intra-group comparisons were statistically different ($p<0.05$).
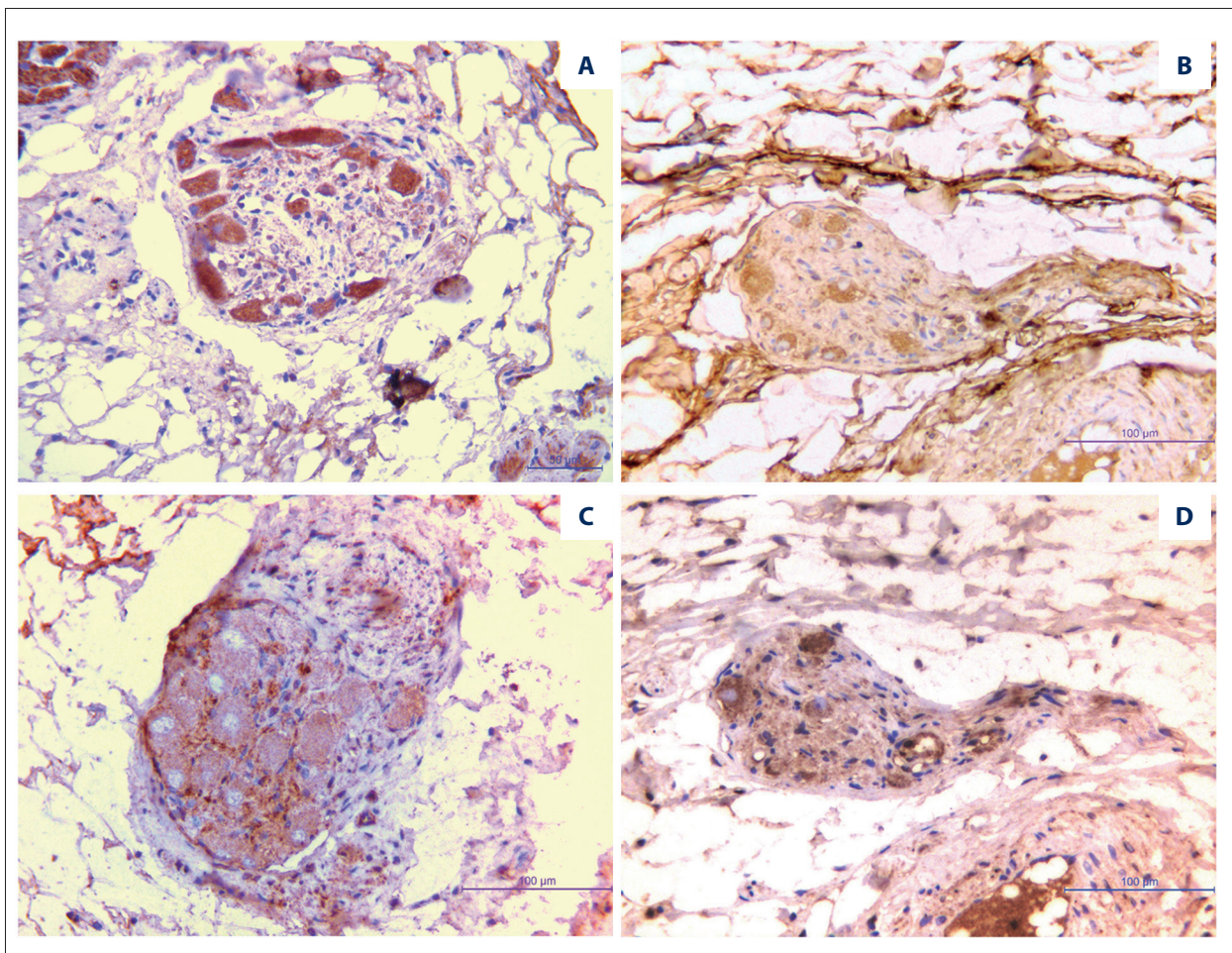
Figure 6. Comparison of choline acetyl transferase and neurturin in ARGP between the control group and the rapid atrial pacing group. Blue is the nucleus, brown is positive staining. (**A**) Choline acetyl transferase staining of ARGP for the sham-operation control group. (**B**) Choline acetyl transferase staining of ARGP for the rapid atrial pacing group. (**C**) Neurturin staining of ARGP for the sham-operation group. (**D**) Neurturin staining of ARGP for the rapid atrial pacing group.

The pacing group choline acetyl transferase ARGP/the sham-operation choline acetyl transferase ARGP=(65.48±7.80)×1,000 μm²/mm²/(30.32±5.65)×1,000 μm²/mm²=2.15. The pacing group choline acetyl transferase IRGP/the sham-operation choline acetyl transferase IRGP=(69.31±7.45)×1,000 μm²/mm²/(28.40±6.30)×1,000 μm²/mm²=2.44. The pacing group choline acetyl transferase SLGP/the sham-operation choline acetyl transferase

SLGP=$(67.78\pm7.24)\times1,000$ μm²/mm²/$(27.56\pm3.58)\times1,000$ μm²/mm²=2.46. The pacing group choline acetyl transferase ILGP/the sham-operation choline acetyl transferase ILGP=$(65.30\pm6.83)\times1,000$ μm²/mm²/$(31.87\pm4.13)\times1,000$ μm²/mm²=2.05.

In the sham-operation group, the density of neurturin (neurotropic factor derived by glia) immunoreactive neurons in the ARGP, IRGP, SLGP, and ILGP were $(22.33\pm3.55)\times1,000$ μm²/mm², $(25.46\pm4.57)\times1,000$ μm²/mm², $(24.47\pm3.56)\times1,000$ μm²/mm², and $(22.87\pm4.32)\times1,000$ μm²/mm², respectively. In the rapid atrial pacing group, the density of neurturin immunoreactive neurons in the ARGP, IRGP, SLGP, and ILGP were $(45.57\pm3.20)\times1,000$ μm²/mm², $(46.35\pm4.63)\times1,000$ μm²/mm², $(46.54\pm2.45)\times1,000$ μm²/mm², and $(47.30\pm4.41)\times1,000$ μm²/mm², respectively. The difference in choline acetyl transferase positive neuron density between the control and rapid atrial pacing groups was significantly different ($p<0.05$, see Figures 6 and 7).

Discussion

Atrial fibrillation improves GP activity

The existence of cardiac GP was first described by Lazzara et al. and proposed in a study by Randall et al., where it was shown that various GP independently constituted an epicardial or local atrial neural network, creating the so-called "brain of the heart." Moreover, they demonstrated that there was mutual communication and influence between each GP [18,19]. GP are surrounded by a fat pad composed of epicardial fat and ligament, and their activity is closely related to atrial activity [20,21]. Previously, many studies have found that GP are distributed around the pulmonary vein ostium, where nerve fiber density is much higher relative to the distal end. Furthermore, it has been observed clinically that stimulating GP in atrial fibrillation patients can promote focal electrical activity in the pulmonary vein or the junction of the pulmonary vein and atrium. Consequently, damage of the GP network could also reveal inhibition of atrial fibrillation onset and progression. Taken together, these studies demonstrate a functional role for GP in the occurrence and persistence of atrial fibrillation [22–25]. Meanwhile, the coexistence of adrenergic and cholinergic nerves in GP and which nerve exhibited stronger activity during atrial fibrillation remained unclear.

We found using immunohistochemistry that GP are composed of various ganglia. Staining for tyrosine hydroxylase and choline acetyl transferase overlapped, which is consistent with the idea that cholinergic and adrenergic substances coexist within the same GP ganglion. There were also cells that secreted cholinergic and adrenergic substances in some of the cells' endochylema. Overall, the dominant nerve distributed in atrial GP was the cholinergic nerve, potentially explaining why vagal effects were observed clinically when GP were stimulated during radiofrequency ablation operations. Second, intragroup comparisons demonstrated that expression of both tyrosine hydroxylase and choline acetyl transferase in the rapid atrial pacing group was higher than the control group. This indicated that the adrenergic and cholinergic nerves were simultaneously activated after atrial fibrillation and that the activity of GP was high, demonstrating a close relationship between atrial fibrillation and GP. GP activity improved during pacing induced atrial fibrillation, and, conversely, improved GP activity induced more incidents of atrial fibrillation.

Imbalanced cardiac autonomic nervous system induces the occurrence and persistence of atrial fibrillation

Activity of the heart is regulated by the adrenergic and cholinergic nerves, and studies have shown that combined adrenergic and cholinergic activity of cardiac autonomic nervous system can induce atrial fibrillation [26,27]. The cardiac autonomic nervous system is closely related to paroxysmal atrial fibrillation, and it plays a key role in the occurrence and termination of atrial fibrillation. Conversely, persistence of atrial fibrillation influences the level of the tension of autonomic nerves during the occurrence and termination of atrial fibrillation. Given the effect they have on each other, a vicious cycle is created [28–30]. Often in clinical studies, paroxysmal atrial fibrillation patients show fluctuations of the level of the tension in autonomic nerves prior to atrial fibrillation occurrence. Adrenergic nerve activity increases for a few minutes before atrial fibrillation onset, followed by an increase in cholinergic nerve activity. Usually, activity of the heart is regulated by the adrenergic and cholinergic nerves. When adrenaline modulates the activity of the heart, the regulation of cholinergic activity weakens, the converse is also true. Therefore, adrenergic and cholinergic innervation of the heart can be balanced. Our experiments showed that both adrenergic and cholinergic nerve activity increased in the absence of atrial fibrillation, but not the one's activity increased and the other's activity decreased. Therefore, we hypothesized that there was imbalance of adrenergic and cholinergic innervation of the heart during atrial fibrillation. These findings suggest that dysregulation and imbalance of autonomic nervous function are key factors regulating the occurrence and persistence of atrial fibrillation.

Nerve growth factor is an essential mediator of nerve growth and differentiation, and its expression level determines the density of the adrenergic nerve. Neurturin is a neurotrophic factor involved in neural plasticity and may promote the extension of cholinergic neuritis. Consequently, it is possible that neurturin may positively regulate growth, proliferation, and differentiation of the cholinergic nerve. In this study, immunohistochemical staining for nerve growth factor and neurturin revealed

that the number of immunoreactive cells for nerve factor and neurturin in GP was greater in the rapid atrial pacing group than the control group. Since atrial fibrillation promoted the proliferation and differentiation of adrenergic and cholinergic nerves, and increases in atrial fibrillation duration increased the incidence of atrial fibrillation; it follows that both adrenergic and cholinergic nerves were likely activated during atrial fibrillation. This ultimately caused imbalance in the automatic nervous system, and this simultaneous activation of the adrenergic and cholinergic nerves resulted in arrhythmia. This imbalance also readily causes the occurrence and persistence of atrial fibrillation.

Limitations

One limitation of our work was that we did not examine the dynamic changes of nerve discharge. If these GP discharges had been recorded, as was done by Yu et al. [31], our understanding of the mechanisms underlying the occurrence and persistence of atrial fibrillation in neural activity would have been better characterized. In addition, sodium pentobarbital enhanced adrenergic activity and inhibited the sympathomimetic effect of the cholinergic nerve, influencing the results to some extent. And, finally, we only performed semi-quantitative analysis of immunohistochemistry, thereby limiting our ability to interpret the data from a molecular biology perspective.

Clinical correlate

Based on our findings, the specificity of GP and the imbalance of the automatic nervous system during atrial fibrillation are better understood. This new knowledge adds to a growing body of evidence that will facilitate the use of denervation treatment to improve the success rate of pulmonary vein circumferential ablation in paroxysmal atrial fibrillation patients. Such a therapy will provide long-term benefits to atrial fibrillation patients.

Conclusions

Incremental excitability of both the adrenergic and cholinergic nerves led to an increase in the frequency of atrial fibrillation incidents, suggesting that there exists an imbalance of autonomic nerve factors in epicardial ganglionated plexi during acute atrial fibrillation.

Conflict of interest

None.

References:

1. Chugh SS, Havmoeller R, Narayanan K et al: Worldwide epidemiology of atrial fibrillation: A Global Burden of Disease 2010 Study. Circulation, 2014; 129: 837–47

2. Lip GY, Brechin CM, Lane DA: The global burden of atrial fibrillation and stroke: a systematic review of the epidemiology of atrial fibrillation in regions outside North America and Europe. Chest, 2012; 142: 1489–98

3. Zoni-Berisso M, Lercari F, Carazza T, Domenicucci S: Epidemiology of atrial fibrillation: European perspective. Clin Epidemiol, 2014; 6: 213–20

4. Park HW, Shen MJ, Lin SF et al: Neural mechanisms of atrial fibrillation. Curr Opin Cardiol, 2012; 27: 24–28

5. Shen MJ, Choi EK, Tan AY et al: Neural mechanisms of atrial arrhythmias. Nat Rev Cardiol, 2012; 9: 30–39

6. Kapa S, Venkatachalam KL, Asirvatham SJ: The autonomic nervous system in cardiac electrophysiology: An elegant interaction and emerging concepts. Cardiol Rev, 2010; 18: 275–84

7. Scherlag BJ, Po S: The intrinsic cardiac nervous system and atrial fibrillation. Curr Opin Cardiol, 2006; 21: 51–54

8. Armour JA: Potential clinical relevance of the 'little brain' on the mammalian heart. Exp Physiol, 2008; 93: 165–76

9. Lo LW, Scherlag BJ, Chang HY et al: Paradoxical long-term proarrhythmic effects after ablating the "head station" ganglionated plexi of the vagal innervation to the heart. Heart Rhythm, 2013; 10: 751–57

10. Po SS, Nakagawa H, Jackman WM: Localization of left atrial ganglionated plexi in patients with atrial fibrillation. J Cardiovasc Electrophysiol, 2009; 20: 1186–89

11. Scherlag BJ, Yamanashi W, Patel U et al: Autonomically induced conversion of pulmonary vein focal firing into atrial fibrillation. J Am Coll Cardiol, 2005; 45: 1878–86

12. Schauerte P, Scherlag BJ, Pitha J et al: Catheter ablation of cardiac autonomic nerves for prevention of vagal atrial fibrillation. Circulation, 2000; 102: 2774–80

13. Lu Z, Scherlag BJ, Lin J et al: Autonomic mechanism for initiation of rapid firing from atria and pulmonary veins: Evidence by ablation of ganglionated plexi. Cardiovasc Res, 2009; 84: 245–52

14. Katritsis DG, Pokushalov E, Romanov A et al: Autonomic denervation added to pulmonary vein isolation for paroxysmal atrial fibrillation: A randomized clinical trial. J Am Coll Cardiol, 2013; 62: 2318–25

15. Pokushalov E, Romanov A, Katritsis DG et al: Ganglionated plexus ablation vs. linear ablation in patients undergoing pulmonary vein isolation for persistent/long-standing persistent atrial fibrillation: A randomized comparison. Heart Rhythm, 2013; 10: 1280–86

16. Lu Z, Scherlag BJ, Lin J et al: Atrial fibrillation begets atrial fibrillation: Autonomic mechanism for atrial electrical remodeling induced by short-term rapid atrial pacing. Circ Arrhythm Electrophysiol, 2008; 1: 184–92

17. Zhou J, Scherlag BJ, Edwards J et al: Gradients of atrial refractoriness and inducibility of atrial fibrillation due to stimulation of ganglionated plexi. J Cardiovasc Electrophysiol, 2007; 18: 83–90

18. Lazzara R, Scherlag BJ, Robinson MJ, Samet P: Selective in situ parasympathetic control of the canine sinoatrial and atrioventricular nodes. Circ Res, 1973; 32: 393–401

19. Randall WC, Kaye MP, Thomas JX, Barber MJ: Intrapericardial denervation of the heart. J Surg Res, 1980; 29: 101–9

20. Zhang Y, Scherlag BJ, Lu Z et al: Comparison of atrial fibrillation inducibility by electrical stimulation of either the extrinsic or the intrinsic autonomic nervous systems. J Interv Card Electrophysiol, 2009; 24: 5–10

21. Hou Y, Scherlag BJ, Lin J et al: Interactive atrial neural network: Determining the connections between ganglionated plexi. Heart Rhythm, 2007; 4: 56–63

22. Lin J, Scherlag BJ, Niu G et al: Autonomic elements within the ligament of Marshall and inferior left ganglionated plexus mediate functions of the atrial neural network. J Cardiovasc Electrophysiol, 2009; 20: 318–24

23. Katritsis D, Giazitzoglou E, Sougiannis D et al: Complex fractionated atrial electrograms at anatomic sites of ganglionated plexi in atrial fibrillation. Europace, 2009; 11: 308–15

24. Yu L, Scherlag BJ, Dormer K et al: Autonomic denervation with magnetic nanoparticles. Circulation, 2010; 122: 2653–59

25. Yu L, Scherlag BJ, Sha Y, Li S et al: Interactions between atrial electrical remodeling and autonomic remodeling: How to break the vicious cycle. Heart Rhythm, 2012; 9: 804–9

26. Patterson E, Po SS, Scherlag BJ, Lazzara R: Triggered firing in pulmonary veins initiated by *in vitro* autonomic nerve stimulation. Heart Rhythm, 2005; 2: 624–31

27. Tan AY, Zhou S, Ogawa M et al: Neural mechanisms of paroxysmal atrial fibrillation and paroxysmal atrial tachycardia in ambulatory canines. Circulation, 2008; 118: 916–25

28. Shen MJ, Zipes DP: Role of the autonomic nervous system in modulating cardiac arrhythmias. Circ Res, 2014; 114: 1004–21

29. Liu Y, Scherlag BJ, Fan Y et al: Experimental model of focal atrial tachycardia: Clinical correlates. J Cardiovasc Electrophysiol, 2013; 24: 909–13

30. Malcolme-Lawes LC, Lim PB, Wright I et al: Characterization of the left atrial neural network and its impact on autonomic modification procedures. Circ Arrhythm Electrophysiol, 2013; 6: 632–40

31. Yu L, Scherlag BJ, Li S et al: Low-level vagosympathetic nerve stimulation inhibits atrial fibrillation inducibility: Direct evidence by neural recordings from intrinsic cardiac ganglia. J Cardiovasc Electrophysiol, 2011; 22: 455–63